UCSF

Title

Abnormal age-related cortical folding and neurite morphology in children with developmental dyslexia

Permalink

https://escholarship.org/uc/item/8rd14920

Journal

NEUROIMAGE-CLINICAL, 18

ISSN

2213-1582

Authors

Caverzasi, E
Mandelli, ML
Hoeft, F
et al.

Publication Date

2018

DOI

10.1016/j.nicl.2018.03.012

Peer reviewed

Abnormal age-related cortical folding and neurite morphology in children with developmental dyslexia

Eduardo Caverzasi[a,b,c,*], Maria Luisa Mandelli[a,d], Fumiko Hoeft[a,e], Christa Watson[a,d], Marita Meyer[a], Isabel E. Allen[f], Nico Papinutto[b], Cheng Wang[a,d,e], Claudia A.M. Gandini Wheeler-Kingshott[g,h,i], Elysa J. Marco[b,e,j], Pratik Mukherjee[k], Zachary A. Miller[a,d], Bruce L. Miller[b,d], Robert Hendren[a,e], Kevin A. Shapiro[a,b], Maria Luisa Gorno-Tempini[a,d]

[a] Dyslexia Center, University of California, San Francisco, San Francisco, CA, USA
[b] Department of Neurology, University of California, San Francisco, San Francisco, CA, USA
[c] Biomedical Sciences PhD, Department of Brain and Behavioral Sciences, University of Pavia, Pavia, Italy
[d] Memory and Aging Center, Department of Neurology, University of California, San Francisco, San Francisco, CA, USA
[e] Department of Psychiatry and Weill Institute for Neurosciences, University of California, San Francisco, San Francisco, CA, USA
[f] Department of Epidemiology and Biostatistics, University of California, San Francisco, San Francisco, CA, USA
[g] Queen Square MS Centre, Department of Neuroinflammation, UCL Institute of Neurology, Russel Square House, London, United Kingdom
[h] Department of Brain and Behavioral Sciences, University of Pavia, Pavia, Italy
[i] Brain MRI 3T Mondino Research Center, C. Mondino National Neurological Institute, Pavia, Italy
[j] Department of Pediatrics, University of California, San Francisco, San Francisco, CA, USA
[k] Neuroradiology Section, Department of Radiology and Biomedical Imaging, University of California, San Francisco, USA

ABSTRACT

There is increasing recognition of a relationship between regional variability in cerebral gyrification and neurodevelopment. Recent work in morphometric MRI has shown that the local gyrification index (lGI), a measure of regional brain folding, may be altered in certain neurodevelopmental disorders. Other studies report that the lGI generally decreases with age in adolescence and young adulthood; however, little is known about how these age-dependent differences in brain maturation occur in atypical neurodevelopment and mechanisms underlying gyrification, such as synaptic pruning. Organization and optimization of dendrites and axons connections across the brain might be driving gyrification and folding processes. In this study, we first assessed lGI differences in the left hemisphere in a cohort of 39 children with developmental dyslexia (DD) between the ages of 7 and 15 years in comparison to 56 typically developing controls (TDC). To better understand the microstructural basis of these changes, we next explored the relationship between lGI differences and cortical thickness and neurite morphology by applying neurite orientation dispersion and density imaging (NODDI). We identified significant differences in lGI between children with DD and TDC in left lateral temporal and middle frontal regions. Further, DD failed to show the expected age-related decreases in lGI in the same regions. Age-related differences in lGI in DD were not explained by differences in cortical thickness, but did correlate with NODDI neurite density and orientation dispersion index. Our findings suggest that gyrification changes in DD are related to abnormal neurite morphology, and are possibly an expression of differences in synaptic pruning.

1. Introduction

Developmental dyslexia (DD) is characterized by unexpectedly low reading ability despite normal general intelligence and educational exposure (Giraud and Ramus, 2013). While the underlying biological basis of dyslexia is not fully understood, many genes associated with dyslexia have been shown to affect neural migration in the neocortex (Giraud and Ramus, 2013), and postmortem studies have demonstrated migrational abnormalities including cortical ectopias and focal microgyri (Galaburda, 1985; Galaburda et al., 1985).

Cortical development is a complex process that begins in the early weeks of pregnancy and lasts through adolescence and early adulthood,

driven by an interaction between genetic and environmental factors (Lenroot and Giedd, 2008). Cortical maturation in the early years reflects a combination of volume growth and cortical folding (gyrification) (White et al., 2010), which allows for a dramatic increase in cortical surface area (Zilles et al., 1988; Zilles et al., 2013). Although the major sulci and gyri are well established by around 2 years of age, developmental changes occurring throughout childhood are likely to shape and further modify local folding patterns (White et al., 2010). Novel morphometric MRI techniques allow in vivo three-dimensional evaluation of folding patterns by computing the local gyrification index (lGI), defined as the amount of cortical surface buried within the sulcal folds compared with the amount of visible cortex in circular regions of interest (Schaer et al., 2012). One study evaluating lGI in typically developing children indicated that there is a decrease in lGI during late childhood/adolescence (Klein et al., 2014). These changes in lGI only partially overlapped with modifications in thickness and volume, suggesting that the observed decrease in lGI is a relatively independent phenomenon and might be related to ongoing microstructural modification within the cerebral cortex (Beck and Yaari, 2008; Vandermosten et al., 2015).

Recent evidence from neuroimaging suggests that some neurodevelopmental disorders, such as autism spectrum disorder and attention deficit-hyperactivity disorder, are associated with atypical cortical folding (Ecker et al., 2016; Fairchild et al., 2015; Mous et al., 2014). A few recent neuroimaging studies have also identified lGI anomalies in children with DD (Im et al., 2016; Williams et al., 2018). However, none of these studies has explicitly examined how age impacts gyrification patterns differently in individuals with DD as compared to typically developing peers. Indeed, cortical maturation and folding are dynamic processes that continue through childhood and adolescence, as described above (Klein et al., 2014).

Furthermore, structural MRI approaches alone do not shed light on the neurobiological processes that underlie atypical folding and lGI changes. Novel advanced diffusion MRI imaging models may contribute to the understanding of the microscopic processes underlying the macroscopic structural morphometric differences between children with DD and their typically developing peers. In particular, neurite orientation dispersion and density imaging (NODDI) allows us to identify and characterize microstructural features of neurites contributing to the diffusion signal (Caverzasi et al., 2016; Zhang et al., 2012). NODDI provides two key metrics, the neurite density and the orientation dispersion indexes, that characterize the microstructural organization of neurons' dendritic projections and axons (neurites) (Grussu et al., 2017). Neurites comprise the computational circuitry of the brain. NODDI allows the quantification of neurite morphology (density and orientation distribution), which changes over the lifespan and is tightly linked to functional efficiency (Tariq et al., 2016). Specifically, development of brain function is associated with increased dispersion of the neurite orientation distribution. The level of complexity of neurite morphology, and in particular of dendritic arborization (dendritic density), has been shown to mediate the role played by cortical regions in several cognitive functions (Jacobs et al., 2001).

In this study, we assessed differences in local gyrification between children with a diagnosis of DD and age-matched control children and how these alterations are related to age. We hypothesized that there would be between-group differences in local gyrification in region of the language network implicated in DD. We also applied a multimodal approach combining lGI, cortical thickness, and NODDI data to investigate the microstructural changes underlying differences in gyrification.

2. Material and methods

2.1. Subjects

Subjects with prior clinical diagnoses of DD were recruited from a

private school for students with dyslexia, the UCSF Pediatric Brain Center, and local schools. Typically developing control (TDC) participants were recruited through local schools, online parent group servers and referrals from the affiliated UCSF Sensory Neurodevelopment and Autism Program (Chang et al., 2015).

All DD subjects were native and fluent speakers of English between 7 and 15 years of age. They were evaluated by a multidisciplinary team, including a behavioral neurologist, psychiatrist and neuropsychologist. They also underwent a detailed clinical interview and neurological examination. All DD had prior formal diagnoses of dyslexia, no general intellectual disability (global cognitive estimates fell at or above the 9th percentile of same-aged peers) and at least one current reading score falling below the 25th percentile of same-aged peers on a standardized measure of reading (Woodcock-Johnson, TOWRE or GORT; see Section 2.2 below), despite extensive school-based reading intervention. The 25th percentile was selected to increase sensitivity because these are students who were previously identified as having dyslexia but have now received significant reading interventions. Exclusion criteria included acquired brain injury, neurological disorders such as perinatal injuries, seizures and severe migraine. Subjects with primary psychiatric diagnoses, such as autism spectrum disorder, major depression, severe generalized anxiety and bipolar disorder were also excluded from the study. Subjects with co-occurrence of DD and attention-deficit/hyperactivity disorder (ADHD) were included.

The TDC group had no history of academic difficulties, no prior diagnoses of DD, nor developmental, neurological or psychiatric disorders. Subjects with a general cognitive estimate below the 9th percentile were excluded, same as in the DD population. Furthermore, reading was formally tested in 19 TDC subjects and scores below the 16th percentile (−1 SD from the mean) were considered as exclusion criteria.

All subjects underwent MRI with high resolution structural and diffusion data within six months of cognitive evaluation. MR sequences required for neurite orientation dispersion and density imaging (NODDI) implementation were added to our protocol during the course of the study, and are therefore only available on a subset of the sample.

One hundred subjects met all inclusion criteria. Five subjects were excluded due to incomplete or poor quality MRI scans. A total of 39 children with DD (mean age 9.9, SD 2.1 years ranging from 7 to 15, 19F, 33 right handed) and 56 age-matched TDC children (age 10.1, SD 1.4 years ranging from 7 to 13; 17F, all right handed) were included in the final analysis. NODDI dedicated images were acquired in a subgroup of 21 TDC and 26 DD (Table 1).

Ten (25.6%) of the DD cohort also had a diagnosis of ADHD, consistent with population co-morbidity estimates (Germano et al., 2010). More than half (60%) of the DD cohort was recruited from a single local school specialized in teaching students with language-based learning differences.

Guardians of the participants provided written informed consent, and participants provided assent. The study was approved by the UCSF Committee on Human Research.

2.2. Neuropsychological and academic assessment

Children with DD underwent neuropsychological and academic

Table 1
Demographics of the entire TDC and DD groups as well as the subgroups, who underwent NODDI protocol study #.

	Analysis	N	F:M	Age mean ± SD; range
TDC	LGI	56	17:39	10.01 ± 1.4; 7–13
	# NODDI	21	9:12	10 ± 1.79; 7–13
DD	LGI	39	19:20	9.9 ± 2.1; 7–15
	# NODDI	26	13:13	10.04 ± 1.87; 7–13

testing administered by research staff or neuropsychology fellows, who were trained and supervised by neuropsychologists. Neuropsychological testing covered screening of nonverbal reasoning (WASI Matrix Reasoning), processing speed (NEPSY II Naming, Children Colored Trails, WISC-IV Integrated Symbol Search and Coding), attention and working memory (WISC-IV Integrated Digit and Spatial Span), verbal and visual recall (California Verbal Learning Test - Children's Version, Rey-Osterrieth Copy and Immediate Recall), visuo-spatial abilities (abbreviated Judgment of Line Orientation, Beery-Buktenica Test of Visual-Motor Integration), and executive functioning (NEPSY II Word Generation and Inhibition and Switching, DKEFS Design Fluency, Children Colored Trails) (Delis et al., 1994; Korkman et al., 2007; Llorente et al., 2003; Meyers and Meyers, 1995; Wechsler, 2004). Academic testing was performed using the Woodcock-Johnson IV (WJ-IV) (Schrank et al., 2014). In addition to the untimed single-word reading measures included in the WJ-IV, participants also completed the timed Test of One-Word Reading Efficiency, Version 2 (TOWRE-2) (Torgesen et al., 2012) and the Gray Oral Reading Test (GORT) (Wiederholt and Bryant, 2012), which evaluates paragraph reading. Due to limitations of time, protocol updates, or subject fatigue, not all subjects with DD were able to complete all of the tests (see Table 2). Nineteen TDC subjects underwent screening cognitive (WASI Matrix Reasoning) and single-word reading (TOWRE-2) tests as part of our study. The remaining 37 TDC participants underwent full-scale intelligence quotient (IQ) testing as part of another study at our institution, as described in (Chang et al., 2015). Both TDC groups did not report any history of learning disabilities or academic difficulties.

2.3. MRI acquisition

All subjects underwent MRI acquisition on a 3 T Siemens Trio scanner (Siemens, Erlangen, Germany). The protocol included 1) T1-weighted three-dimensional sagittal Magnetization Prepared Rapid Acquisition Gradient Echo (MPRAGE) sequence with the following parameters: $TR/TE/TI = 2300/2.98/900$ ms, $1 \times 1 \times 1$ mm^3 voxel size, field of view (FOV): $256 \times 240 \times 176$ mm^3, flip angle = 9 deg, parallel imaging acceleration factor (iPAT) = 2; 2) axial high angular resolution diffusion-weighted imaging (HARDI) with 64 directions at $b = 2000$ s/mm^2, phase encoding = anterior-posterior, $TR/TE = 8200/86$ ms, $2.2 \times 2.2 \times 2.2$ mm^3 voxel size, FOV: 220×220 mm^2, 60 contiguous slices, flip angle = 9 deg, iPAT 2, including 10 volumes without diffusion-weighting (b0 images), one of which was acquired using a reversed phase-encoding direction (posterior to anterior). The latter allowed estimation and correction for susceptibility-induced distortions; 3) in order to implement the NODDI analysis, an additional diffusion-weighted acquisition was added to the protocol with 30 directions at $b = 700$ s/mm^2 and all other parameters identical to the HARDI sequence described above. This additional sequence was acquired only in a subgroup of subject (see Section 2.1) Total acquisition time of the DWI data was approximately 17 min.

Table 2
Non-verbal intelligence estimate, and reading scores of a subset of the dyslexic cohort and typically developing control participants. Age is in years (mean [SD]); reading, language, and cognitive scores are reported in percentiles (mean [SD]).

	Percentile scores	
	DD children	TDC children
Matrix Reasoning (n = 39 DD; 19 TDC)	70.97 [23.73]	76.82 [16.38]
TOWRE SWE (n = 30 DD; 19 TDC)	18.53 [20.94][a]	62.00 [23.91]
TOWRE PDE (n = 30 DD; 19 TDC)	15.27 [12.26][a]	61.95 [22.27]
GORT Rate (n = 30 DD; 19 TDC)	24.58 [19.96]	N/A
GORT Accuracy (n = 24 DD)	13.21 [13.40]	N/A
GORT Fluency (n = 24 DD)	17.50 [13.73]	N/A
GORT Comprehension (n = 24 DD)	25.08 [19.52]	N/A

[a] Statistically significant different in DD compared to TDC.

2.4. FreeSurfer-based analysis and lGI

The preprocessing of T1-weighted images was carried out using FreeSurfer version 5.3 (http://surfer.nmr.mgh.harvard.edu/) in accordance with a standard auto-reconstruction algorithm, which involved non-uniform intensity normalization, removal of non-brain tissue, affine registration to the Montreal Neurological Institute (MNI) space and Talairach transformation, and segmentation of gray/white matter tissue (Dale et al., 1999; Fischl et al., 1999a; Fischl et al., 1999b). A trained neuroradiologist (EC) visually inspected the segmentation results. Cortical parcellation and thickness measurement were performed by using the Desikan-Kyliany Atlas comprising of 34 cortical volumes of interest per hemisphere (Desikan et al., 2006). Gyrification of the entire cortex was also assessed using FreeSurfer. A 3-D local gyrification index (lGI) was computed using the method described by Schaer et al. (2012) and Schaer et al. (2008). A study-specific template was created based on all 95 subjects and the FreeSurfer dataset was resampled to the average space (Schaer et al., 2012). The results were smoothed with a full-width at half maximum (FWHM) of 5 mm for lGI (Klein et al., 2014).

2.5. NODDI analysis

First, susceptibility-induced off-resonance fields were estimated from the pairs of images acquired with reversed phase-encoding directions (i.e., with distortions in opposite directions) in a way analogous to what is described in Andersson et al.'s (2003) paper. This correction of diffusion data was performed using the "topup" tool of FMRIB Software Library [FSL] (Smith et al., 2004). In addition, eddy current-induced distortions and head motions were estimated and corrected using eddy_correct from the same toolbox; b-vectors were rotated accordingly to account for the corrections.

Neurite orientation dispersion and density imaging (NODDI) model was applied to the pre-processed data (http://mig.cs.ucl.ac.uk/index.php?n=Tutorial.NODDImatlab). The NODDI toolbox decomposes each voxel signal into three compartments (extra-neurite, intra-neurite, and isotropic Gaussian diffusion) and calculates neurite density index (NDI) and orientation dispersion index (ODI) maps (Caverzasi et al., 2016; Zhang et al., 2012). These metrics provide information about the density of the neurites and degree of dispersion of the fiber orientation (ranging from 0 to 1, perfectly coherent to fully dispersed, respectively). We then registered the FreeSurfer parcellation to the diffusion space using bbregister tool of FreeSurfer (https://surfer.nmr.mgh.harvard.edu/fswiki/bbregister). Average NDI and ODI values were extracted within the 34 regions of interest per hemisphere of the cortical parcellation.

2.6. Statistical analysis

We used Pearson's chi-squared test or univariate ANOVA to assess differences in demographics and cognitive scores.

Group-wise lGI imaging statistical analyses were performed using FreeSurfer QDEC 1.5 (query, design, estimate, contrast) software. QDEC fits a general linear model (GLM) at each surface vertex to explain lGI. Local gyrification index/thickness differences between DD and TDC were examined including age as continuous covariates and accounting for gender. To adjust for multiple comparisons, false discovery rate (FDR) was applied at a threshold of $P = 0.05$. Since functional and structural brain alterations in individuals with DD have been primarily observed in left hemisphere (Linkersdorfer et al., 2012; Richlan et al., 2013), we restricted our analysis of sulcal pattern to left hemispheric regions only. In order to check the effect of ADHD diagnosis on our results, analyses were also conducted excluding DD participants with ADHD.

Finally, we performed a least squares regression analysis to study the relationship of lGI with demographic data, thickness, and NODDI

metrics (ODI and NDI). The interaction of diagnosis with each MRI variable was also examined, in order to assess differences in correlation between DD and TDC. Least squares analysis were primarily performed in the regions which showed group-related abnormal lGI values from the FreeSurfer (QDEC) analysis, as well as at the left precentral gyrus used as a control region. In this study, we refer to the control region as a region outside the language network that has shown reductions in lGI values in typically developing subjects during childhood/adolescence (Klein et al., 2014). This region was used to investigate specificity of imaging changes (lGI, and NODDI related metrics) to the language network in DD.

3. Results

3.1. Demographic and psychometric characteristics

There were no significant differences in age, gender or global cognitive estimates between DD and TDC groups (P > 0.05). There was a statistically significant difference in handedness (P = 0.01) between the two cohorts, with a larger proportion of non-right-handed individuals in the DD group. There was also an expected difference in TOWRE scores for a subgroup of DD (n = 30) and TDC (n = 19) scores (P < 0.0001), which follows from the inclusion and exclusion criteria (Table 2). There was no statistically significant difference in demographic data between the whole sample and the subset that underwent the neuropsychological evaluation or the subset that underwent additional NODDI dedicated imaging. Data regarding the cognitive function assessment on the remaining TDC is reported in a recent paper by Chang et al. (2015).

3.2. FreeSurfer-based analysis: local gyrification index

We found a statistically significant increase in lGI in DD compared to TDC (P < 0.05) in several regions of the left hemisphere (Table 3). This difference was due to DD showing no significant reduction in lGI with age, which led to a significantly different correlation between lGI and age in DD compared to TDC (controlling for gender) (P < 0.05) in clusters of the left middle frontal and temporal regions (Table 3) (Fig. 1). The largest cluster, in the left rostral middle frontal gyrus (extending to the caudal portion of the middle frontal lobe), was the only one that survived after FDR correction. Additional analysis was also performed by excluding the 10 DD participants with ADHD and the same statistically significant clusters were confirmed; however, likely due to reduced power these did not survive FDR correction. Both DD and TDC groups showed a statistically significant inverse correlation (P < 0.05) between age and lGI in several clusters belonging to the rolandic (precentral and postcentral gyri), occipital and frontal regions.

3.3. FreeSurfer-based analysis: thickness

DD showed a statistically significant reduced thickness compared to TDC (P < 0.05) in several small clusters scattered throughout the left hemisphere (not shown). Only the clusters in the left superior frontal and lingual gyri remained significant after adjusting for multiple comparisons using FDR correction. These clusters did not overlap with the results of lGI analysis.

3.4. Relationship between gyrification, neurite density and fiber dispersion

We examined the relationship between lGI and demographic data, thickness, and NODDI metrics (ODI, NDI), within clusters showing significant differences in lGI in DD as well as in the precentral gyrus (control region). The least squares regression model of left rostral middle frontal gyrus was statistically significant (P = 0.004) explaining the lGI variability with an R-square of 0.57. Thickness (P = 0.01), gender (P = 0.02), and ODI (P = 0.001) all covaried with lGI. ODI however, was the only index that showed a significant interaction with diagnosis (Fig. 2). Specifically, in the rostral middle frontal gyrus, lGI and ODI least square slope was positive (+0.6) in DD and negative (−0.3) in the control group (Fig. 2). The least squares regression model of the left middle temporal gyrus was also statistically significant (P = 0.0002), explaining the lGI variability with an R-square of 0.70. Gender (P < 0.0001) and NDI (P = 0.02) all covaried with lGI. NDI however, was the only index that showed a significant interaction with diagnosis (Fig. 3). Specifically, in the middle temporal gyrus, lGI and NDI least square slope was positive (+0.4) in DD and negative (−0.6) in the control group (Fig. 3).

Finally, the least squares regression model of the left fusiform gyrus was statistically significant (P = 0.003) explaining lGI variability with an R-square of 0.49. Gender and thickness showed a statistically significant interaction with diagnosis. No statistically significant models were identified for the left bank of the superior temporal sulcus, inferior temporal or precentral gyri lGI (P > 0.05).

4. Discussion

In this study, we identified local differences in gyrification in left frontal and temporal brain regions between children with developmental dyslexia and typically developing peers. Specifically, unlike the control group in this work and previous studies on typically developing children, our DD group did not show an expected age-related decrease in lGI in these regions. Differences in lGI were related to measures of neurite morphology, both in terms of density of neurites and their orientation dispersion. There was a difference between developmental dyslexia and typically developing control participants in the interaction between lGI and NODDI metrics, which suggests that the lGI changes in DD may be related to abnormal neurite organization, affecting specific regions in selective ways.

There is increasing recognition of a relationship between regional variability in cerebral gyrification and differences in cognition and neurodevelopment (Ecker et al., 2016; Fairchild et al., 2015; Klein et al., 2014; Mous et al., 2014). This is not surprising if we consider the crucial phylogenetic role of brain folding, which leads to a dramatic increase in cortical surface and gray matter by lateral expansion, while still allowing for the development of an efficient and sustainable network of connections across the brain (White et al., 2010). It has been shown that this degree of connectivity would not be practically achievable in any other way, such as by thickening the cortical layers (vertical expansion) (Murre and Sturdy, 1995).

Gyrification events occurring during fetal development have been studied using in vivo imaging as well as post-mortem examination (Chi et al., 1977; White et al., 2010). During these early stages of primary and secondary folding, genetic factors are thought to play a predominant role. Nevertheless, changes in gray and white matter

Table 3
Results from lGI analysis result. Clusters showing both a statistically significant increase in lGI in DD compared to TDC as well as a statistically significant difference in correlation between lGI and age between the two groups. Cluster significance is noted as −log10(P). Number of vertex per each cluster and its coordinates in the MNI space are also reported.

Left hemisphere clusters	P	No. of vertices	MNIx	MNIy	MNIz
Rostral middle frontal gyrus[a]	−4.04	1454	−42.7	17.9	39.3
Bank of the superior temporal sulcus	−3.1	522	−53.7	−42.5	−4.8
Middle temporal gyrus	−2.71	296	−58.5	−51	−8.7
Inferior temporal gyrus	−2.57	113	−56.6	−48.9	−25.1
Fusiform gyrus	−2.29	54	−37.6	−19.8	−28.6

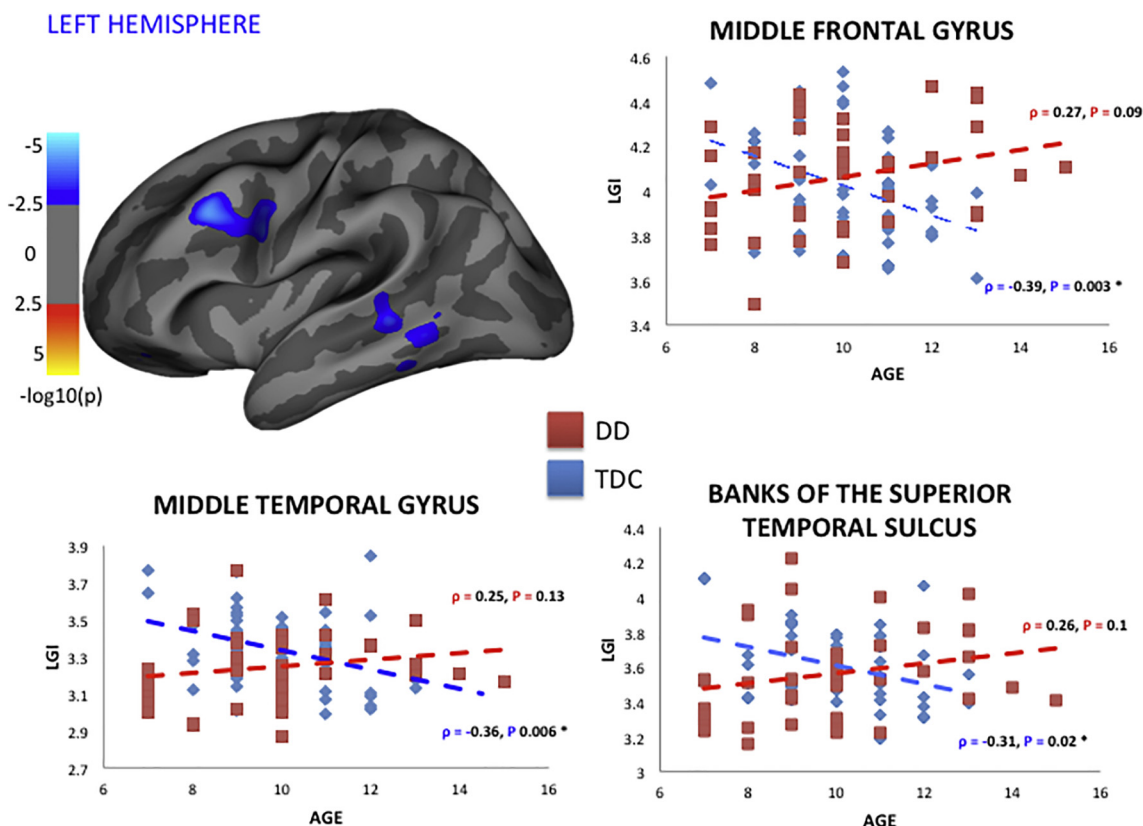[a] Area surviving the FDR correction (P < 0.05).

Fig. 1. Results of the local gyrification index analysis comparing healthy subjects to DD in the left hemisphere. In the top left the figure shows clusters of regions having a statistically significant difference in correlation between lGI and age compared to TDC. Clusters are overlaid to an inflated brain volume shown on a lateral view. The map is -log10(P), where P is the significance, so a Min of 2 will display all vertices with P < 0.01 and a Max of 5 will show vertices of P < 0.0001 as the same color. Scatter plots of three representative clusters are also shown. Age is reported on the x-axis, whereas lGI values are represented on the y-axis for healthy (blue) and DD (red) subjects. Spearman r and P values for the age and lGI correlation are also reported and marked with "*" once statistically significant (P < 0.05). In dyslexic children there was a lack of inverse correlation between age and lGI: lGI seems not to reduce with age as observed and described in literature. The same clusters showed a statistically significant increased lGI in DD compared to healthy subjects. (For interpretation of the references to colour in this figure legend, the reader is referred to the web version of this article.)
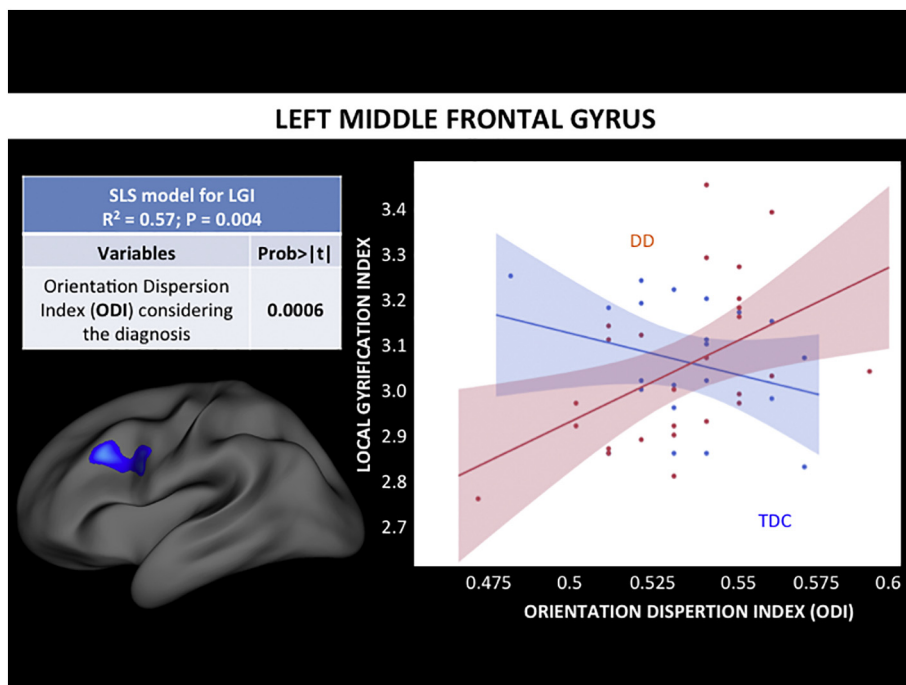

Fig. 2. Standard least square analysis results in the left rostral middle frontal gyrus. We performed a least squares (LS) regression analysis to study the relationship between lGI, other demographics, and MRI metrics: we modeled the variability of lGI by ODI controlling for age, gender, thickness, NDI, and diagnosis. The interaction of diagnosis with each MRI variable was also examined, in order to assess differences in correlation between DD and TDC. We identified statistically significant (P = .004) model explaining the left rostral middle frontal gyrus lGI with R-squared of 0.57. In particular thickness and gender seemed to be informative, as well as ODI, however the latter only once considering the different diagnosis. In the rostral middle frontal gyrus, lGI and ODI seem to be directly correlated in DD, whereas not correlated or slightly inversely correlated in TDC.
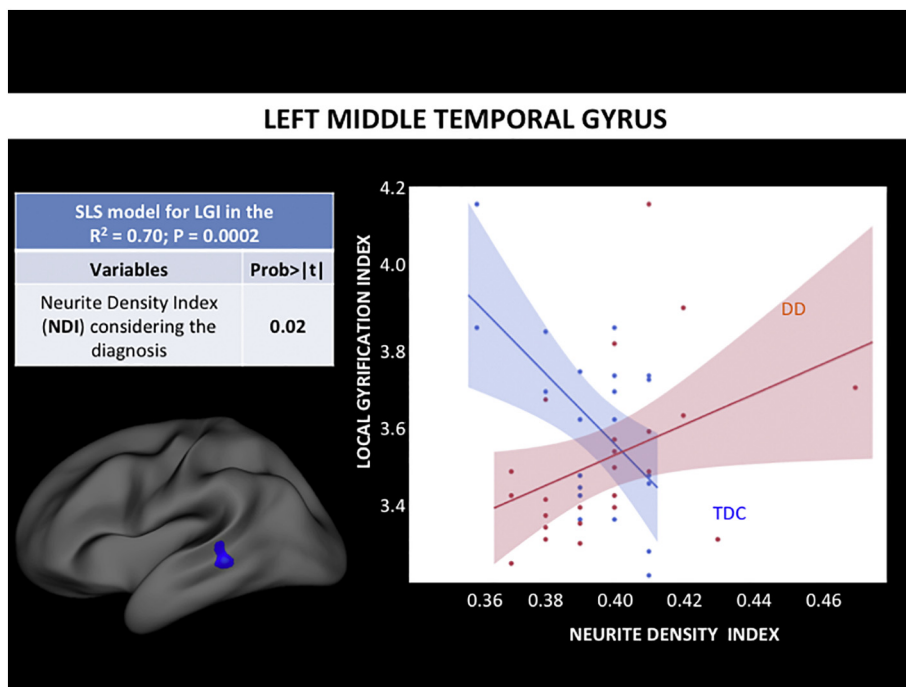
Fig. 3. Standard least square analysis results in the left bank of the posterior temporal sulcus. We performed a least squares (LS) regression analysis to study the relationship between lGI, other demographics, and MRI metrics: we modeled the variability of lGI by ODI controlling for age, gender, thickness, NDI, and diagnosis. The interaction of diagnosis with each MRI variable was also examined, in order to assess differences in correlation between DD and TDC. We identified a statistically significant (P = 0.0002) model explaining the left middle temporal gyrus lGI with R-squared of 0.70. Gender, thickness and NDI were informative, however, the latter two only after considering the different diagnosis. In particular NDI and lGI seem to be directly related to DD, whereas inversely related in the TDC group.

structure continue to occur throughout childhood and adolescence up to early adulthood, re-shaping and modifying local patterns of gyrification (White et al., 2010). Recent work in morphometric MRI has shown that gyrification indices are not stable in the course of adolescence and young adulthood, and the lGI generally decreases with age in frontal and temporal brain regions (Klein et al., 2014). This tertiary folding is still related to genetic factors, but it is also likely influenced by experience-dependent brain changes (Klein et al., 2014; White et al., 2010).

Some recent imaging studies have suggested that there may be gyrification anomalies in DD (Im et al., 2016; Plonski et al., 2017; Williams et al., 2018). Specifically, pre- and early beginning readers with familial risk/history of DD (Im et al., 2016) and children with DD (Im et al., 2016; Williams et al., 2018) showed abnormal lGI values in left temporo-parietal and temporo-occipital regions compared to typically developing subjects. This was in line with previous structural and functional MRI studies that identified morphometric abnormalities (Richlan et al., 2013; Xia et al., 2016) and hypoactivation (Linkersdorfer et al., 2012; Raschle et al., 2012) in the same posterior brain regions. Another recent multicenter study of children and adolescents with dyslexia identified lGI abnormalities not only in left posterior language-related regions (superior and middle temporal gyri), but also in prefrontal areas. By applying a machine learning approach, they identified geometric properties of the left hemisphere cortex (folding and mean curvature) as features that best discriminated between DD and control children (Plonski et al., 2017).

These previous gyrification findings in DD have been interpreted as reflecting abnormal processes of sulcation and folding in early development, i.e., the fetal and neonatal periods, and do not take into account of the relationship between lGI and age/development (Klein et al., 2014). Consistent with what Klein and colleagues reported, our control group showed a progressive reduction of lGI during childhood in several brain regions. In our DD group, on the other hand, we demonstrated the absence of this age-related decrease in lGI of left fronto-temporal regions, specifically in the left middle-frontal gyrus and in the posterior portion of the left temporal lobe. These areas are involved in reading, as well as being part of the larger language-processing network (Price, 2010; Silani et al., 2005).

We can interpret our lGI and NODDI neuroimaging results in view of

the hypothesized relationship between cortical folding and structural white matter connectivity (Van Essen, 1997). Specifically, gyrification might be strongly driven by the optimization of white matter connections within the brain, as tension-mediated forces along the axons tend to bring highly connected regions closer to each other. In the early years of life, abnormal neuronal migration could lead to abnormal structural white matter connectivity and therefore gyrification abnormalities, such as the ones described by Im and colleagues in left parieto-temporal and occipito-temporal regions of early beginning readers with familial risk/history of DD (Im et al., 2016). Our lGI results showed abnormalities in different regions in the frontal and temporal cortex in older children with DD. Our findings that lGI changes in DD were explained by NODDI-related metrics provide some evidence regarding the relationship between cortical morphology and white matter organization. Therefore, the reported NODDI analysis suggests an association between cortical folding changes that occur during childhood and adolescence and ongoing microstructural reorganization of neurite morphology. Interestingly, a recent study linked gray matter neuroanatomy and white matter structural connectivity to explain developmental anomalies in autistic children (Ecker et al., 2016). Specifically increased lGI in the rolandic cortical region was associated with increased axial diffusivity in the underlying subcortical white matter. Therefore the anomalous lGI pattern in DD might be driven by atypical maturation of neurite morphology, and could also potentially become a target or "marker" for early intervention in DD.

The microanatomical and neurobiological bases of DD are still debated. Here we speculate on possible neural substrates of our neuroimaging findings. The differences in gyrification within language-related regions in our cohort may be the expression of genetic influences, as downstream effects of vulnerabilities in the developing language network. On the other hand, they could also be related to experience-dependent brain changes occurring during the course of language and reading acquisition (or lack thereof). There is ample evidence that white matter microstructure is altered by experience, and that synaptic pruning and modification of the dendritic arborization play a major role in the optimization and increased efficiency of brain networks in this stage of neurodevelopment (Schlaggar and McCandliss, 2007; White et al., 2010). Perhaps the most likely interpretation of these findings is that they represent an interaction between genetic differences and

experience. It is unlikely that the findings solely reflect lack of experience, since many of the children in our DD cohort had received extensive language-based interventions. However, it may be the case that children with DD have an atypical neurobiological response to reading, resulting in differences in experience-dependent anatomical changes.

The main limitations of the study are the relatively small cohort of DD subjects, and the fact that only a subset of them underwent NODDI dedicated imaging, likely resulting in differential correlation of its two metrics with lGI. Nevertheless, our unique multimodal imaging approach allowed us to suggest novel insights that will need to be confirmed by future longitudinal studies.

5. Conclusions

We used a multimodal neuroimaging approach to show that school-age children with DD show differences in age-dependent gyrification in left frontal and temporal regions crucial for language and reading skills. We demonstrate for the first time a correlation between lGI changes and abnormal neurite morphology (as assessed by NODDI), which may suggest that differences in synaptic pruning contribute to neuroanatomical changes in developmental dyslexia. This study highlights the usefulness of a multimodal approach to understanding neuroimaging and neural changes in DD.

Acknowledgement

References

Andersson, J.L., Skare, S., Ashburner, J., 2003. How to correct susceptibility distortions in spin-echo echo-planar images: application to diffusion tensor imaging. NeuroImage 20, 870–888.

Beck, H., Yaari, Y., 2008. Plasticity of intrinsic neuronal properties in CNS disorders. Nat. Rev. Neurosci. 9, 357–369.

Caverzasi, E., Papinutto, N., Castellano, A., Zhu, A.H., Scifo, P., Riva, M., Bello, L., Falini, A., Bharatha, A., Henry, R.G., 2016. Neurite Orientation Dispersion and Density Imaging color maps to characterize brain diffusion in neurologic disorders. J. Neuroimaging 26, 494–498.

Chang, Y.S., Gratiot, M., Owen, J.P., Brandes-Aitken, A., Desai, S.S., Hill, S.S., Arnett, A.B., Harris, J., Marco, E.J., Mukherjee, P., 2015. White matter microstructure is associated with auditory and tactile processing in children with and without sensory processing disorder. Front. Neuroanat. 9, 169.

Chi, J.G., Dooling, E.C., Gilles, F.H., 1977. Gyral development of the human brain. Ann. Neurol. 1, 86–93.

Dale, A.M., Fischl, B., Sereno, M.I., 1999. Cortical surface-based analysis. I. Segmentation and surface reconstruction. NeuroImage 9, 179–194.

Delis, D., Kramer, J., Kaplan, E., Ober, B., 1994. California Verbal Learning Test children's Version. Psychological Assessment Resources. Inc., California.

Desikan, R.S., Segonne, F., Fischl, B., Quinn, B.T., Dickerson, B.C., Blacker, D., Buckner, R.L., Dale, A.M., Maguire, R.P., Hyman, B.T., Albert, M.S., Killiany, R.J., 2006. An automated labeling system for subdividing the human cerebral cortex on MRI scans into gyral based regions of interest. NeuroImage 31, 968–980.

Ecker, C., Andrews, D., Dell'Acqua, F., Daly, E., Murphy, C., Catani, M., Thiebaut de Schotten, M., Baron-Cohen, S., Lai, M.C., Lombardo, M.V., Bullmore, E.T., Suckling, J., Williams, S., Jones, D.K., Chiocchetti, A., Consortium, M.A., Murphy, D.G., 2016. Relationship between cortical gyrification, white matter connectivity, and autism spectrum disorder. Cereb. Cortex 26, 3297–3309.

Fairchild, G., Toschi, N., Hagan, C.C., Goodyer, I.M., Calder, A.J., Passamonti, L., 2015. Cortical thickness, surface area, and folding alterations in male youths with conduct disorder and varying levels of callous-unemotional traits. Neuroimage Clin. 8, 253–260.

Fischl, B., Sereno, M.I., Dale, A.M., 1999a. Cortical surface-based analysis. II: inflation, flattening, and a surface-based coordinate system. NeuroImage 9, 195–207.

Fischl, B., Sereno, M.I., Tootell, R.B., Dale, A.M., 1999b. High-resolution intersubject averaging and a coordinate system for the cortical surface. Hum. Brain Mapp. 8, 272–284.

Galaburda, A.M., 1985. Developmental dyslexia: a review of biological interactions. Ann. Dyslexia 35, 19–33.

Galaburda, A.M., Sherman, G.F., Rosen, G.D., Aboitiz, F., Geschwind, N., 1985.

Developmental dyslexia: four consecutive patients with cortical anomalies. Ann. Neurol. 18, 222–233.

Germano, E., Gagliano, A., Curatolo, P., 2010. Comorbidity of ADHD and dyslexia. Dev. Neuropsychol. 35, 475–493.

Giraud, A.L., Ramus, F., 2013. Neurogenetics and auditory processing in developmental dyslexia. Curr. Opin. Neurobiol. 23, 37–42.

Grussu, F., Schneider, T., Tur, C., Yates, R.L., Tachrount, M., Ianuş, A., Yiannakas, M.C., Newcombe, J., Zhang, H., Alexander, D.C., DeLuca, G.C., Gandini Wheeler-Kingshott, C., 2017. Neurite dispersion: a new marker of multiple sclerosis spinal cord pathology? Ann. Clin. Transl. Neurol. 4, 663–679.

Im, K., Raschle, N.M., Smith, S.A., Ellen Grant, P., Gaab, N., 2016. Atypical sulcal pattern in children with developmental dyslexia and at-risk kindergarteners. Cereb. Cortex 26, 1138–1148.

Jacobs, B., Schall, M., Prather, M., Kapler, E., Driscoll, L., Baca, S., Jacobs, J., Ford, K., Wainwright, M., Treml, M., 2001. Regional dendritic and spine variation in human cerebral cortex: a quantitative golgi study. Cereb. Cortex 11, 558–571.

Klein, D., Rotarska-Jagiela, A., Genc, E., Sritharan, S., Mohr, H., Roux, F., Han, C.E., Kaiser, M., Singer, W., Uhlhaas, P.J., 2014. Adolescent brain maturation and cortical folding: evidence for reductions in gyrification. PLoS One 9, e84914.

Korkman, M., Kirk, U., Kemp, S., 2007. NEPSY–Second Edition (NEPSY-II). The Psychological Corporation, San Antonio, TX.

Lenroot, R.K., Giedd, J.N., 2008. The changing impact of genes and environment on brain development during childhood and adolescence: initial findings from a neuroimaging study of pediatric twins. Dev. Psychopathol. 20, 1161–1175.

Linkersdörfer, J., Lonnemann, J., Lindberg, S., Hasselhorn, M., Fiebach, C.J., 2012. Grey matter alterations co-localize with functional abnormalities in developmental dyslexia: an ALE meta-analysis. PLoS One 7, e43122.

Llorente, A., Williams, J., Satz, P., D'Elia, L., 2003. Children's Color Trails Test (CCTT). Psychological Assessment Resources, Odessa, Florida.

Meyers, J.E., Meyers, K.R., 1995. Rey Complex Figure Test and Recognition Trial Professional Manual. Psychological Assessment Resources.

Mous, S.E., Karatekin, C., Kao, C.Y., Gottesman, I.I., Posthuma, D., White, T., 2014. Gyrification differences in children and adolescents with velocardiofacial syndrome and attention-deficit/hyperactivity disorder: a pilot study. Psychiatry Res. 221, 169–171.

Murre, J.M., Sturdy, D.P., 1995. The connectivity of the brain: multi-level quantitative analysis. Biol. Cybern. 73, 529–545.

Plonski, P., Gradkowski, W., Altarelli, I., Monzalvo, K., van Ermingen-Marbach, M., Grande, M., Heim, S., Marchewka, A., Bogorodzki, P., Ramus, F., Jednorog, K., 2017. Multi-parameter machine learning approach to the neuroanatomical basis of developmental dyslexia. Hum. Brain Mapp. 38, 900–908.

Price, C.J., 2010. The anatomy of language: a review of 100 fMRI studies published in 2009. Ann. N. Y. Acad. Sci. 1191, 62–88.

Raschle, N.M., Zuk, J., Gaab, N., 2012. Functional characteristics of developmental dyslexia in left-hemispheric posterior brain regions predate reading onset. Proc. Natl. Acad. Sci. U. S. A. 109, 2156–2161.

Richlan, F., Kronbichler, M., Wimmer, H., 2013. Structural abnormalities in the dyslexic brain: a meta-analysis of voxel-based morphometry studies. Hum. Brain Mapp. 34, 3055–3065.

Schaer, M., Cuadra, M.B., Tamarit, L., Lazeyras, F., Eliez, S., Thiran, J.P., 2008. A surface-based approach to quantify local cortical gyrification. IEEE Trans. Med. Imaging 27, 161–170.

Schaer, M., Cuadra, M.B., Schmansky, N., Fischl, B., Thiran, J.P., Eliez, S., 2012. How to measure cortical folding from MR images: a step-by-step tutorial to compute local gyrification index. J. Vis. Exp. e3417.

Schlaggar, B.L., McCandliss, B.D., 2007. Development of neural systems for reading. Annu. Rev. Neurosci. 30, 475–503.

Schrank, F.A., Mather, N., McGrew, K.S., 2014. Woodcock-Johnson IV Tests of Achievement. Riverside, Rolling Meadows, IL.

Silani, G., Frith, U., Demonet, J.F., Fazio, F., Perani, D., Price, C., Frith, C.D., Paulesu, E., 2005. Brain abnormalities underlying altered activation in dyslexia: a voxel based morphometry study. Brain 128, 2453–2461.

Smith, S.M., Jenkinson, M., Woolrich, M.W., Beckmann, C.F., Behrens, T.E., Johansen-Berg, H., Bannister, P.R., De Luca, M., Drobnjak, I., Flitney, D.E., Niazy, R.K., Saunders, J., Vickers, J., Zhang, Y., De Stefano, N., Brady, J.M., Matthews, P.M., 2004. Advances in functional and structural MR image analysis and implementation as FSL. NeuroImage 23 (Suppl. 1), S208–219.

Tariq, M., Schneider, T., Alexander, D.C., Gandini Wheeler-Kingshott, C.A., Zhang, H., 2016. Bingham-NODDI: mapping anisotropic orientation dispersion of neurites using diffusion MRI. NeuroImage 133, 207–223.

Torgesen, J., Wagner, R., Rashotte, C., 2012. TOWRE-2: Test of Word Recognition Efficiency–Examiner Manual. Pro-Ed, Austin, TX.

Van Essen, D.C., 1997. A tension-based theory of morphogenesis and compact wiring in the central nervous system. Nature 385, 313–318.

Vandermosten, M., Vanderauwera, J., Theys, C., De Vos, A., Vanvooren, S., Sunaert, S., Wouters, J., Ghesquiere, P., 2015. A DTI tractography study in pre-readers at risk for dyslexia. Dev. Cogn. Neurosci. 14, 8–15.

Wechsler, D., 2004. WISC-IV: Wechsler Intelligence Scale for Children, Integrated: Technical and Interpretive Manual. Harcourt Brace and Company.

White, T., Su, S., Schmidt, M., Kao, C.Y., Sapiro, G., 2010. The development of gyrification in childhood and adolescence. Brain Cogn. 72, 36–45.

Wiederholt, J., Bryant, B., 2012. Gray Oral Reading Test–Fifth Edition (GORT-5): Examiner's Manual. Pro-Ed, Austin, TX.

Williams, V.J., Juranek, J., Cirino, P., Fletcher, J.M., 2018. Cortical thickness and local gyrification in children with developmental dyslexia. Cereb. Cortex 28, 963–973.

Xia, Z., Hoeft, F., Zhang, L., Shu, H., 2016. Neuroanatomical anomalies of dyslexia:

disambiguating the effects of disorder, performance, and maturation. Neuropsychologia 81, 68–78.

Zhang, H., Schneider, T., Wheeler-Kingshott, C.A., Alexander, D.C., 2012. NODDI: practical in vivo neurite orientation dispersion and density imaging of the human brain. NeuroImage 61, 1000–1016.

Zilles, K., Armstrong, E., Schleicher, A., Kretschmann, H.J., 1988. The human pattern of gyrification in the cerebral cortex. Anat. Embryol. 179, 173–179.

Zilles, K., Palomero-Gallagher, N., Amunts, K., 2013. Development of cortical folding during evolution and ontogeny. Trends Neurosci. 36, 275–284.